J. Fluid Mech. (1996), *vol.* 325, *pp.* 1–28

Active sonic boom control

By STEVEN C. CROW AND GENE G. BERGMEIER
Aerospace and Mechanical Engineering Department, The University of Arizona, Tucson, AZ 85721, USA

(Received 5 December 1995 and in revised form 14 May 1996)

A theory and simulation code are developed to study non-steady sources as means to control sonic booms of supersonic aircraft. A key result is that the source of sonic boom pressure is not confined to the length of the aircraft but occupies an extensive segment of the flight path. An aircraft in non-steady flight functions as a synthetic aperture antenna, generating complex acoustic waves with no simple relation to instantaneous volume or lift distributions.

The theory applies linear acoustics to slender non-steady sources but requires no far-field approximation. The solution for pressure contains a term not seen in Whitham's theory for sonic booms of distant supersonic aircraft. The term describes a pressure field that decays algebraically behind the Mach cone and, in the case of steady flight, integrates to a ground load equal to the weight of the aircraft. The algebraic term is separate from those that describe the sonic boom.

Two non-steady source phenomena are evaluated: periodic velocity changes (surge), and periodic longitudinal lift redistribution (slosh). Surge can attenuate a sonic boom and covert it into prolonged weak reverberation, but accelerations needed to produce the phenomenon seem too large for practical use. Slosh may be practical and can alter sonic booms but does not, on average, result in boom attenuation. The conclusion is that active sonic boom abatement is possible in theory but maybe not practical.

1. Introduction

This is a study of sonic booms produced by aircraft in non-steady flight. Our goal was to find whether non-steady source phenomena can scramble or attenuate sonic booms heard by listeners on the ground. Such source phenomena would constitute active sonic boom control, similar to the active methods recently developed to control sound in enclosures.

A freely propagating sonic boom is very different than sound in an enclosure. Active sound control methods work best on sound fields in small enclosures or on sources near resonance, but neither condition applies to sonic booms. Active sonic boom control must somehow prevent the pressure waves generated by a supersonic aircraft from coalescing into compact and coherent waves at large distances. The control method must work for listeners located anywhere on the ground. A method that reduces sound at specific locations but increases it elsewhere could not be considered successful.

Pioneers of sonic boom theory were Landau (1945), Hayes (1954), and Whitham (1956). They developed a model of sonic booms that has guided thinking for forty years and has produced many accurate predictions. Figure 1(*a*) illustrates a few aspects of that model. An aircraft flying at a steady supersonic speed produces local flow perturbations, which can be treated by linear compressible flow theory if the perturbations are not too large. The perturbations evolve outward from the flight path on Mach cones, the characteristic surfaces of the underlying compressible flow

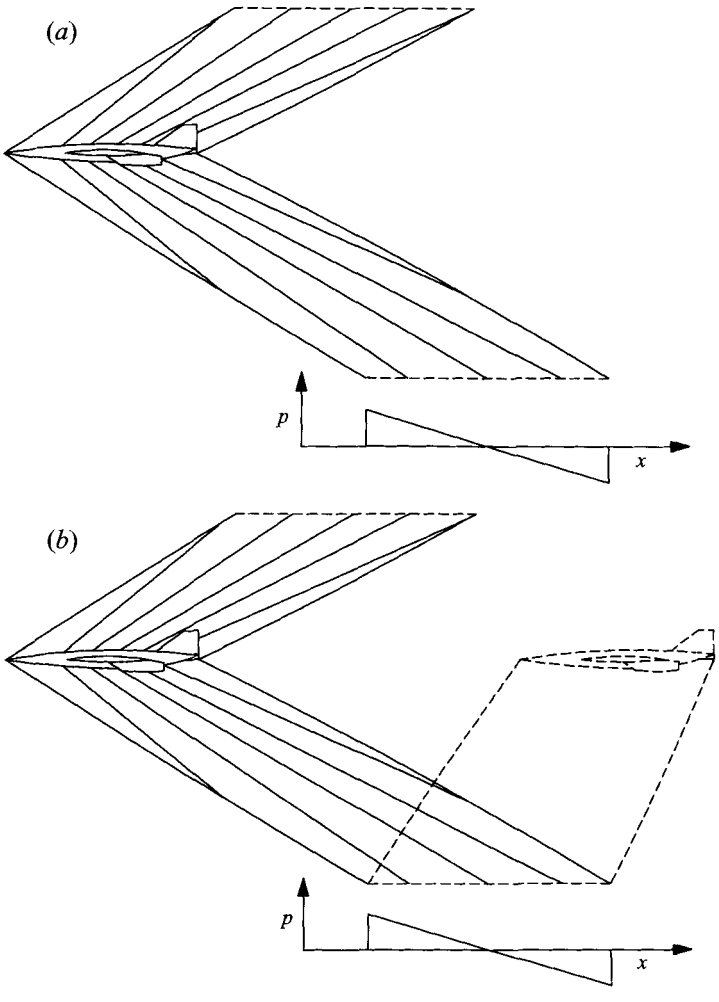

FIGURE 1. (*a*) Sonic boom below an aircraft in steady supersonic flight. The Mach cones signify mathematical but not physical causality. (*b*) Ray model of a sonic boom source. Ray theory handles boom propagation phenomena well, but the phantom aircraft is not a valid source concept.

equations. Linear theory implies that the Mach cones all incline at the same angle, but weak nonlinearities cause the cones to coalesce where pressure increases with distance back along the flight path. The coalesced cones form shock waves, and the shocks absorb more Mach cones until only a simple N-shaped pressure wave remains far from the flight path.

The model of Landau, Hayes, and Whitham has guided thinking about sonic booms for the past forty years. The model implies that sonic booms are likely to be robust, and indeed they are. The processes depicted in figure 1 (*a*) seem inexorable. Each Mach cone seems able to convey information about the local shape of the aircraft outward and downward to the hapless listeners on the ground.

Yet there is a subtle loophole in the classical model of sonic booms. Landau developed the original theory of weakly converging characteristics in the context of signalling problems, where the characteristics really are trajectories of information flow. An example might be an oscillating point source, radiating spherical sound waves. Characteristics can be plotted as lines in coordinates of radius and time, and

each characteristic can convey a message about the source until both characteristic and message are absorbed in a shock.

The characteristic cones of figure 1(*a*) are not characteristic surfaces of the compressible flow equations in three dimensions plus time and are not paths of information flow. They are mathematical conveniences resulting from the assumption that the aircraft is flying steadily. The aircraft in figure 1(*a*) could have ceased to exist, and the N-wave would arrive at the indicated location as though nothing had changed (sounds of disintegration would come later). The sonic boom was created somewhere back along the flight path and reflects flight conditions during some epoch before the instant depicted in the figure.

So where and when was the sonic boom created? A plausible answer involves ray paths, as seen in figure 1(*b*). Ray paths are orthogonal to Mach cones and are lines along which acoustic energy propagates. Perhaps the boom heard at a point on the ground propagated down a ray path that originated on the flight path of the aircraft. The source of the boom was the aircraft at an earlier time, an acoustic image shown as a dashed outline in the figure.

Ray theory, or geometrical acoustics, has played an important role in the study of sonic boom propagation. Most sonic boom prediction codes have combined Whitham's theory of weakly nonlinear wave propagation with ray tracing to account for manoeuvres and atmospheric refraction (Hayes, Haefeli & Kulsrud 1968). Despite its success with propagation phenomena, however, ray theory cannot provide a satisfactory account of the origin of sonic booms. Ray theory is based on a short-wave approximation that fails wherever the acoustic wavelength is comparable to the scale for changes of pressure amplitude. Precisely such conditions prevail close to an aircraft, so the rays cannot be used to follow a sonic boom to its source.

The phantom aircraft of figure 1(*b*) is not the source of the sonic boom. The real source is more like a motion picture segment of the phantom aircraft and occupies a region extended in space and time, usually much longer than the aircraft itself. The extended source can be made to function as a synthetic aperture wave generator, which is why active sonic boom control is worth considering.

An aircraft can be an active acoustic source in two ways: by manoeuvring or by changing shape. Elegant theories have been developed for the effects of large-scale manoeuvres, with emphasis on the formation of 'super booms' where shock waves fold into caustics (Seebass 1970). Those theories involve four modelling stages: linear steady compressible aerodynamics near the source, weakly nonlinear wave propagation, ray theory to locate caustics, and nonlinear transonic flow theory to handle the caustics themselves. Those theories may have some bearing on active control by manoeuvres, but effective active control manoeuvres take place at frequencies too high for steady aerodynamics and ray tracing to apply.

Garrick & Maglieri (1968) conducted flight tests that have a bearing on the possibility of active sonic boom control. Figure 2 is reproduced from their report to illustrate the test conditions. The aircraft was an F106 flying at Mach 1.5 and an altitude of 35000 ft. The pilot subjected the aircraft to a sinusoidal porpoising manoeuvre at a frequency of 1 Hz, with vertical accelerations of ± 0.5 g. Aerodynamic lift must have varied from 0.5 to 1.5 times the weight of the aircraft, so the source strength for the component of sonic boom due to lift varied by a factor of 3.0. Garrick & Maglieri expected the sinusoidal source variation to 'print through' to the ground, producing a sinusoidal boom strength variation with a wavelength around 1500 ft. Notice that the figure shows both characteristics and rays, presumably path options along which the source variations might propagate to the ground.

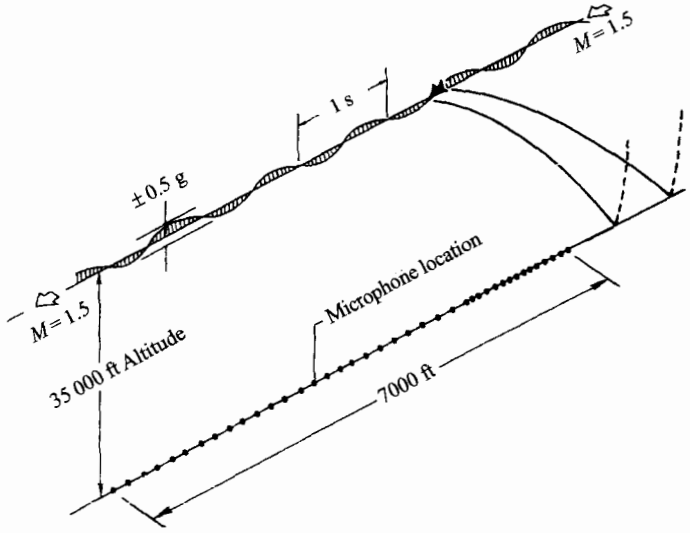

FIGURE 2. Schematic of test arrangements for evaluating the effects of aircraft motion on sonic-boom pressure signatures on the ground (from Garrick & Maglieri 1968).

When the records from the ground-based microphones were processed, they revealed no periodicity whatever near a wavelength of 1500 ft. Instead the wave forms were about as would have been expected for steady flight, with some random variations attributable to atmospheric turbulence (Crow 1969).

The results were a real puzzle at the time, but the theory developed in this paper explains them easily. The sonic boom recorded at any point on the ground did not originate from a single location in the sky, but rather from an interval of several thousand feet along the flight path. Each boom was an average over several cycles of the porpoising manoeuvre.

The relation between an actively controlled source and a sonic boom on the ground can be more complicated than a simple average. Even the simple case of a point source moving steadily and oscillating sinusoidally produces a complex wave form with a spectrum of Doppler-shifted frequencies (Goldstein 1976). The acoustic signature of an aircraft with active sonic boom control will be more complex still.

2. Formulation

Our study of active sonic boom control is based on slender-body theory and linear acoustics. Nonlinear shock formation and propagation may be important, but linear acoustics should provide a useful first look at prospects for active control.

The coordinates for the theory are time t and the three dimensions of space,

$$\boldsymbol{x} = (x, y, z), \tag{2.1}$$

fixed with respect to the atmosphere far from the aircraft. The aircraft flies along the x-axis in the direction of decreasing x. The z-axis points upward, and the y-axis points along the starboard wing. The origin of time is chosen so that the aircraft nose intercepts the origin of coordinates at time zero.

Pressure is the sum of ambient pressure p_0 and a perturbation p,

$$p_0 + p(\boldsymbol{x}, t), \tag{2.2}$$

and density is expressed in similar form:

$$\rho_0 + \rho(\boldsymbol{x}, t). \tag{2.3}$$

The ambient pressure p_0 and density ρ_0 are defined at the altitude of the flight path, while p and ρ are perturbation pressure and density in our notation. The flow velocity $\boldsymbol{u}(\boldsymbol{x}, t)$ is measured relative to the atmosphere far from the aircraft.

Three equations set forth the principles of linear acoustics. They are conservation of mass,

$$\frac{\partial \rho}{\partial t} + \rho_0 \nabla \cdot \boldsymbol{u} = \rho_0 q, \tag{2.4}$$

conservation of momentum,

$$\rho_0 \frac{\partial \boldsymbol{u}}{\partial t} + \nabla p = \boldsymbol{f}, \tag{2.5}$$

and the equation of state for isentropic compression,

$$p = c_0^2 \rho. \tag{2.6}$$

The scalar source on the right of (2.4) represents a distributed volume flow of fluid of ambient density, while the vector source on the right of (2.5) is a distributed body force imposed on unit volumes of fluid. The quantity c_0 in (2.6) is the ambient speed of sound. The distributed sources are used to represent the passage of the aircraft.

The three equations can be combined into an equation for a single scalar variable, either the pressure perturbation or a velocity potential. To obtain an equation for the pressure perturbation, we differentiate (2.4) with respect to time, take the divergence of (2.5), and use (2.6) to eliminate density in favour of pressure. The result is a wave equation for pressure with source terms on the right:

$$\nabla^2 p - \frac{1}{c_0^2} \frac{\partial^2 p}{\partial t^2} = \nabla \cdot \boldsymbol{f} - \rho_0 \frac{\partial q}{\partial t}. \tag{2.7}$$

That equation, with the addition of a nonlinear quadrupole source term, is the basis for the famous theory of aerodynamic sound (Lighthill 1953).

A second and complementary wave equation can be derived by introducing the concept of a distributed body *impulse* $\boldsymbol{i}$, defined by the ordinary differential equation

$$\boldsymbol{f} = \partial \boldsymbol{i} / \partial t. \tag{2.8}$$

A velocity potential ϕ is defined so that

$$\boldsymbol{u} = \frac{\boldsymbol{i}}{\rho_0} + \nabla \phi. \tag{2.9}$$

Impulse is not used much in acoustics but does play a role in classical hydrodynamics (Lamb 1933). In the context of linear acoustics, impulse is simply the integral of body force over all past times. Notice from (2.9) that the velocity field is not entirely potential, but includes a rotational component equal to the ratio of body impulse over density. The rotational component would include trailing vortices laid down by a travelling impulse.

An equation for velocity potential follows a derivation similar to that for pressure. We combine (2.5) and (2.9) to show that

$$\nabla \left(\rho_0 \frac{\partial \phi}{\partial t} + p \right) = 0, \tag{2.10}$$

and the term in brackets is zero if the pressure perturbation and velocity potential decay to zero at infinity. We combine that result with (2.4), (2.6), and (2.8) to obtain a wave equation for velocity potential:

$$\nabla^2\phi - \frac{1}{c_0^2}\frac{\partial^2\phi}{\partial t^2} = q - \frac{1}{\rho_0}\nabla\cdot\boldsymbol{i}. \tag{2.11}$$

Equation (2.11) is useful for calculations of velocity components and wave drag.

The rest of the study is based on solutions of wave equations (2.7) and (2.11). The initial conditions are that the flow was zero in the distant past, and the boundary conditions are that the flow remains zero far from the origin. The source field q and force field $\boldsymbol{f}$ then determine the flow uniquely.

To define the source and force fields, we assume that the aircraft is a slender body such that q and $\boldsymbol{f}$ are concentrated along the x-axis. Slender-body approximations do involve some loss of generality but are consistent with the nature of our study as a first look at active sonic boom control. The essence of slender-body theory is that the sources and forces are delta functions of y and z times functions of x and t that represent the fuselage and wings of the aircraft. The source has the form

$$q = \delta(y)\,\delta(z)\,\mathscr{Q}(x,t), \tag{2.12}$$

where

$$\mathscr{Q} = \frac{\partial \mathscr{S}}{\partial t}(x,t), \tag{2.13}$$

and $\mathscr{S}(x,t)$ is the area of the fuselage cross-section. Equation (2.13) implies that source strength is proportional to the local pulsation rate of the fuselage, an intuitively appealing result, but one that requires some care to prove (Cole 1953).

We assume that the force and impulse vectors are due mainly to lift and are directed along the z-axis. Thus

$$\boldsymbol{f} = \delta(y)\,\delta(z)\,\mathscr{F}(x,t)\,\boldsymbol{e}_z, \tag{2.14}$$

and

$$\boldsymbol{i} = \delta(y)\,\delta(z)\,\mathscr{I}(x,t)\,\boldsymbol{e}_z, \tag{2.15}$$

with

$$\mathscr{F} = \partial\mathscr{I}/\partial t. \tag{2.16}$$

Once the aircraft has passed, $\mathscr{I}$ no longer changes with time and has a residual value equal to the impulse of the vortex wake. $\mathscr{F}$ is related to the distribution of lift $\mathscr{L}$ along the aircraft. If a planar wing is responsible for all lift, then the force on the air is equal and opposite the lift on the wing:

$$\mathscr{F}(x,t) = -\mathscr{L}(x,t), \quad \text{planar wing.} \tag{2.17}$$

We have to be careful about lifting wings or fuselages with non-zero volumes. $\mathscr{F}$ models forces on an infinite volume of fluid with no internal boundary, including fictional fluid within the fuselage. $\mathscr{F}$ has to accelerate the fictional fluid along with real fluid around the aircraft. For a body of revolution, the inertias of the fluid inside and outside are the same, and

$$\mathscr{F}(x,t) = -2\mathscr{L}(x,t), \quad \text{body of revolution.} \tag{2.18}$$

The analyses of this paper use (2.17) except for §7, which compares the pressure derived from non-steady theory with the classical theory for steady flow over an inclined body of revolution (Tsien 1938).

The formulation of the non-steady sonic boom theory is complete. Equations (2.7) and (2.11) are to be solved subject to zero initial and boundary conditions at infinity and to the body force and source fields of (2.12) and (2.14). Aircraft speed and Mach

number play no roles in the formulation but appear in specific selections of $\mathscr{Q}(x,t)$ and $\mathscr{F}(x,t)$. Fundamentally, the theory applies whether the aircraft is flying at subsonic or supersonic speed.

3. Pressure and velocity

Equations (2.7) and (2.11) are linear non-dispersive wave equations with inhomogeneous terms on the right. The simplest version is (2.11) with no body impulse, a wave equation for velocity potential driven by a scalar source field. The solution is a volume integral over all the sources,

$$\phi(\boldsymbol{x},t) = -\int_{\infty} q(\boldsymbol{x}',t')\frac{\mathrm{d}V'}{4\pi R}, \tag{3.1}$$

where R is the distance between a source location $\boldsymbol{x}'$ and the point $\boldsymbol{x}$ where ϕ is evaluated,

$$R = |\boldsymbol{x}-\boldsymbol{x}'|, \tag{3.2}$$

and t' is a retarded time,

$$t' = t - R/c_0. \tag{3.3}$$

Solution of wave equation (2.7) for pressure follows by differentiating and superposing terms of the form (3.1):

$$p(\boldsymbol{x},t) = \rho_0 \int_{\infty} \frac{\partial q}{\partial t'}(\boldsymbol{x}',t')\frac{\mathrm{d}V'}{4\pi R} - \boldsymbol{\nabla}\cdot\int_{\infty} \boldsymbol{f}(\boldsymbol{x}',t')\frac{\mathrm{d}V'}{4\pi R}. \tag{3.4}$$

The integrals are performed over the three dimensions of space, but they simplify greatly when the slender-body approximations for q and $\boldsymbol{f}$ are used. From (2.12) to (2.14),

$$p(\boldsymbol{x},t) = \rho_0 \int_{-\infty}^{\infty} \frac{\partial^2 \mathscr{S}}{\partial t'^2}(x',t')\frac{\mathrm{d}x'}{4\pi R} - \frac{\partial}{\partial z}\int_{-\infty}^{\infty} \mathscr{F}(x',t')\frac{\mathrm{d}x'}{4\pi R}. \tag{3.5}$$

The divergence of the second term on the right simplifies to a derivative on z, because the body force $\boldsymbol{f}$ has a z-component only.

The final step in the solution for pressure is to bring the derivative $\partial/\partial z$ into the second volume integral. The variable z occurs in R and also in the retarded time t', which depends on R through (3.3). Thus

$$p = \rho_0 \int_{-\infty}^{\infty} \frac{\partial^2 \mathscr{S}}{\partial t'^2}\frac{\mathrm{d}x'}{4\pi R} + z\int_{-\infty}^{\infty}\left[\frac{\partial \mathscr{F}/\partial t'}{c_0 R} + \frac{\mathscr{F}}{R^2}\right]\frac{\mathrm{d}x'}{4\pi R}. \tag{3.6}$$

The pressure wave forms presented in this paper are based on (3.6). We could compute pressure at any point and time $(\boldsymbol{x},t)$ but have generally assumed that the listener is located a distance h below the flight path, directly under the origin of coordinates. Thus

$$x = 0 \quad y = 0, \quad z = -h, \tag{3.7}$$

and

$$R = (x'^2 + h^2)^{1/2}. \tag{3.8}$$

At location (3.7), pressure is a function of time:

$$p(0,0,-h,t) = p(t). \tag{3.9}$$

The area and force distributions $\mathscr{S}$ and $\mathscr{F}$ remain functions of (x', t') in the integrands of (3.6).

When the altitude h is more than a few thousand feet, the ambient density ρ_0 increases substantially from the flight path at $z = 0$ at the ground at $z = -h$. The energy flux of a propagating wave tends to be conserved and is proportional to p^2/ρ_0, so the pressure amplitude increases as the square-root of ambient density as the wave propagates to the ground. A second phenomenon that alters a pressure wave is ground reflection, which doubles the amplitude when the ground is firm and smooth. The amplification factor

$$2[\rho_0(0)/\rho_0(-h)]^{1/2} \tag{3.10}$$

allows for both phenomena and has been included in all the pressure signatures presented here. If pressures computed by (3.6) were not multiplied by (3.10), they would appear small to those familiar with measurements of sonic booms on the ground.

Solution of wave equation (2.11) for velocity potential follows much the same line as the solution of (2.7) for pressure perturbation. The fundamental solution (3.1) and some differentiation and superposition produce the formula

$$\phi = -\int_{-\infty}^{\infty} \frac{\partial S}{\partial t'} \frac{\mathrm{d}x'}{4\pi R} - \frac{z}{\rho_0} \int_{-\infty}^{\infty} \left[\frac{\mathscr{F}}{c_0 R} + \frac{\mathscr{I}}{R^2} \right] \frac{\mathrm{d}x'}{4\pi R} \tag{3.11}$$

analogous to (3.6) for pressure. The potential ϕ is a function of (x, t), while the source terms $\mathscr{S}$, $\mathscr{F}$, and $\mathscr{I}$ in the integrals are functions of (x', t').

Velocity is the gradient of (3.11) plus an impulse vector, as seen in (2.9). We have used velocity only to compare formulae for velocity components and wave drag with classical formulae of steady flight. Two velocity components are important for the comparisons: the axial component u along the x-axis, and a radial component v normal to the x-axis. To facilitate calculation of the radial component, a change of coordinates from rectangular (x, y, z) to cylindrical (x, r, θ) is appropriate, with the substitutions

$$y = r\cos\theta, \quad z = r\sin\theta, \tag{3.12}$$

on the right of (3.11). The distance between the source and listener takes the form

$$R = [(x-x')^2 + r^2]^{1/2}, \tag{3.13}$$

and the desired velocity components follow from (2.9):

$$u = \frac{\partial \phi}{\partial x}, \quad v = \frac{\sin\theta}{\rho_0} \frac{\delta(r)}{2\pi r} \mathscr{I}(x, t) + \frac{\partial \phi}{\partial r}. \tag{3.14a, b}$$

The derivatives in (3.14) can be evaluated in a straightforward way from (3.11), and the orders of differentiation and integration exchanged to produce computable formulae for velocity components in non-steady flight. The results, however, are hard to compare with established formulae for the velocity components around a supersonic aircraft (Whitham 1974, p. 225). The reasons are not fundamental, but have to do with the fact that 'judicious integration by parts is used to avoid divergent integrals' in the steady theory (Whitham 1974, p. 221). Parallel judicious integrations are needed to match the outcomes of (3.14) with Whitham's steady-state theory.

To evaluate (3.14*a*), we recognize that the integrands of (3.11) have the form

$$\mathscr{H}(x', x-x', r, t), \tag{3.15}$$

where x' appears explicitly and also in the combination $(x-x')$ through (3.13). Thus

$$\frac{\partial \mathscr{H}}{\partial x} = \frac{\partial \mathscr{H}}{\partial x'} - \frac{\mathrm{d}\mathscr{H}}{\mathrm{d}x'}. \tag{3.16}$$

$\partial\mathscr{H}/\partial x$ is a partial derivative that needs to be evaluated for the axial component of velocity u, and $\mathrm{d}\mathscr{H}/\mathrm{d}x'$ is a total derivative that allows for all dependencies on x' with x, r and t held fixed. An integration by parts can be performed on the term involving $\mathrm{d}\mathscr{H}/\mathrm{d}x'$, with the result that

$$u = -\int_{-\infty}^{\infty} \frac{\partial^2 \mathscr{S}}{\partial x' \partial t'} \frac{\mathrm{d}x'}{4\pi R} - \frac{z}{\rho_0} \int_{-\infty}^{\infty} \left[\frac{\partial \mathscr{F}/\partial x'}{c_0 R} + \frac{\partial \mathscr{I}/\partial x'}{R^2} \right] \frac{\mathrm{d}x'}{4\pi R}. \tag{3.17}$$

Evaluation of the radial component of velocity requires several tricks similar in flavour to (3.16), with the result that

$$v = \frac{1}{4\pi r} \int_{-\infty}^{\infty} \left[\frac{1}{c_0} \frac{\partial^2 \mathscr{S}}{\partial t'^2} + \frac{(x-x')}{R} \frac{\partial^2 \mathscr{S}}{\partial x' \partial t'} \right] \mathrm{d}x' + \frac{\sin\theta\, \delta(r)}{\rho_0 \, 2\pi r} \mathscr{I}(x, t)$$
$$+ \frac{\sin\theta}{4\pi\rho_0} \int_{-\infty}^{\infty} \left\{ \frac{\mathscr{I}}{R^3} + \frac{(x-x')}{R} \left[\frac{\partial \mathscr{F}/\partial x'}{c_0 R} + \frac{\partial \mathscr{I}/\partial x'}{R^2} \right] + \frac{1}{c_0} \left[\frac{\partial \mathscr{F}/\partial t'}{c_0 R} + \frac{\mathscr{F}}{R^2} \right] \right\} \mathrm{d}x'. \tag{3.18}$$

Equations (3.17) and (3.18) are easy to integrate numerically and easy to compare with Whitham's theory of steady supersonic flow about slender axisymmetric bodies.

4. Domain of dependence

The integrals in solution (3.6) for pressure and the corresponding solutions (3.17) and (3.18) for velocity range over all values of x' from negative to positive infinity. To compute the integrals numerically, we need to put limits on the domain of integration. Selecting those limits takes us back to the question posed in the introduction: where and when was the sonic boom created?

In the usual acoustics terminology, the sources depend on the *dummy* variable of integration x' and the *retarded* time t'. We prefer more dignified names from relativity theory, where x' is the *proper* location of a source, and t' is *proper* time. From the vantage of the source, x' and t' are the variables that really matter. The fact that a source at proper location and time $(x', 0, 0, t')$ happens to be heard at $(0, 0, -h, t)$ is no concern of the source!

Figure 3(*a*) shows an aircraft cutting a swath through the plane of proper coordinates (x', t'). The aircraft speed is assumed constant, so its nose traces a straight line through the origin, and its tail traces a parallel line shifted an aircraft length in the x'-direction. The aircraft can generate sound only from a *zone of sources* between the two lines. Not all of the zone of sources can contribute to the sound at a specific location and time below the flight path. Equation (3.3) imposes a functional relation between the proper location x' and time t' of the source. The shape of the function $t'(x')$ happens to be a hyperbola, which we call the *hyperbola of dependence*.

Figure 3(*b*) illustrates the zone of sources and hyperbola of dependence under conditions when the two overlap. Only sources along the segment of the hyperbola within the zone of sources can contribute to sound heard under those conditions. That segment of the hyperbola of dependence answers the question of where and when the sonic boom arose.

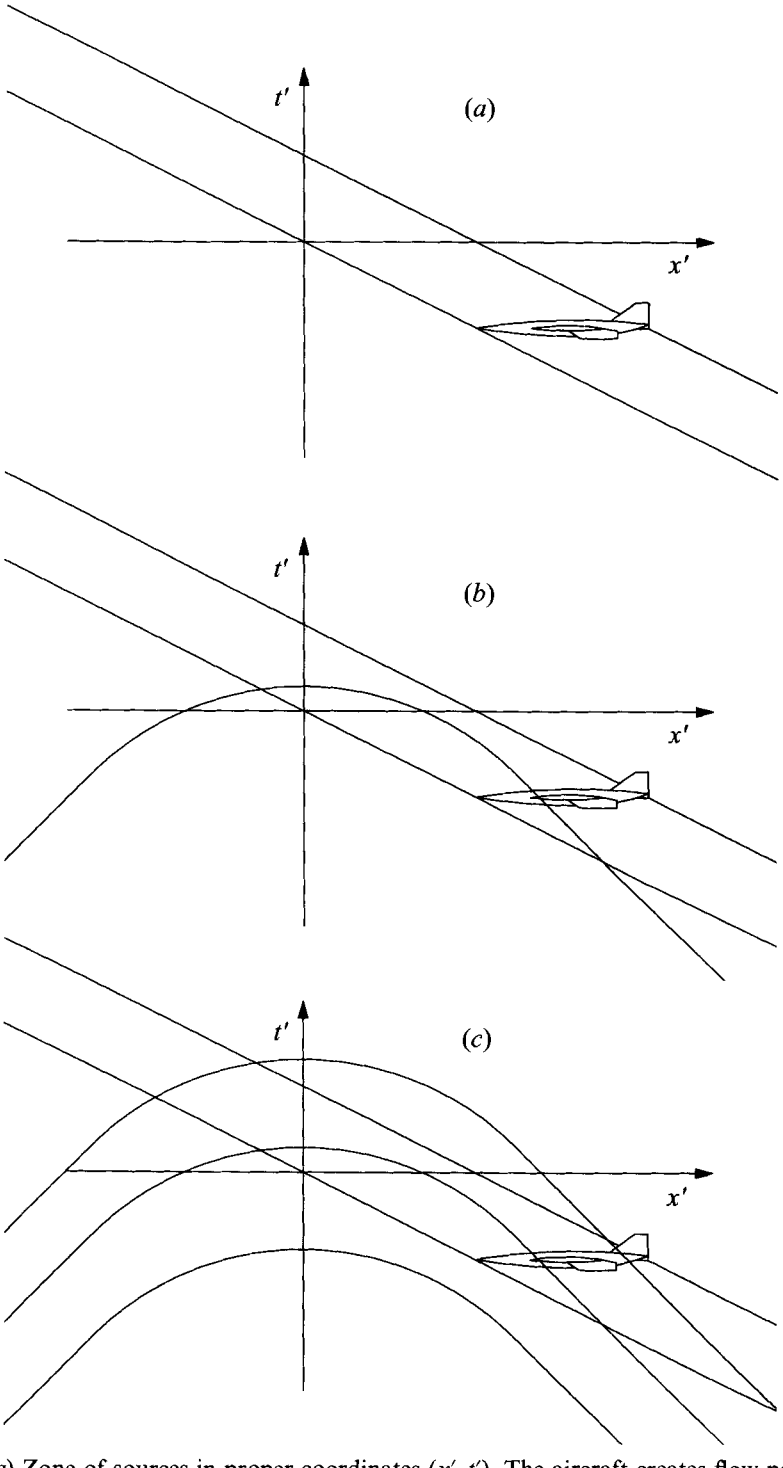

FIGURE 3. (*a*) Zone of sources in proper coordinates (x', t'). The aircraft creates flow perturbations only within the zone of sources. (*b*) Hyperbola of dependence in proper coordinates (x', t'). Only sources along the segment of the hyperbola within the zone of sources contribute to sound at the listener position and time $(0, 0, -h, t)$. (*c*) Upward migration of the hyperbola of dependence with increasing time t.

The nature of the overlap between the hyperbola of dependence and zone of sources depends on aircraft altitude and Mach number and on listener time t. The slope of the lines bounding the zone of sources is $-1/U$, where U is the speed of the aircraft. The asymptotes of the hyperbola of dependence have slopes $\pm 1/c_0$, where c_0 is the speed of sound. The ratio of the two slopes is the Mach number,

$$M = U/c_0. \tag{4.1}$$

When $M < 1$, the zone of sources has a steeper slope than the asymptotes of the hyperbola of dependence. The two always overlap, and they overlap in one segment only. The physical consequence is that the listener always hears a subsonic aircraft, and the acoustic image of the aircraft occupies a single segment of sky. The acoustic image does not coincide with the current location of the aircraft and may be highly elongated.

When $M > 1$, the case shown in the figure, the hyperbola of dependence may overlap the zone of sources not at all, once, or twice, depending on aircraft altitude h and listener time t. Equation (3.3) implies that the hyperbola $t'(x')$ rises along the t'-axis with advancing t, as shown in figure 3(*c*). No overlap occurs at early times, a single segment of overlap occurs at intermediate times, and two segments of overlap occur later. The physical consequences for the supersonic case are that the listener hears nothing for awhile, then hears sources from an elongated but continuous segment of sky, and finally hears sources from two elongated segments of sky, which separate with time.

The path of the aircraft nose in the $(x'\,t')$ plot satisfies the equation

$$t' = -x'/U, \tag{4.2}$$

while (3.3) provides the path of the hyperbola of dependence:

$$t' = t - (x'^2 + h^2)^{1/2}/c_0. \tag{4.3}$$

The two equations are satisfied simultaneously where the hyperbola of dependence intersects the path of the nose, which is the lower boundary of the zone of sources. Equations (4.2) and (4.3) can be combined into a quadratic equation for x', which has one real solution for $M < 0$. For $M > 0$, the quadratic has no real solutions when t is less than the time

$$t_{nose} = (M^2 - 1)^{1/2} h/U \tag{4.4}$$

when sound first reaches the listener from the nose of the aircraft. When $t > t_{nose}$, the quadratic has two solutions

$$x'_{1,4} = \frac{Ut \mp MU(t^2 - t_{nose}^2)^{1/2}}{M^2 - 1}. \tag{4.5}$$

and those are the outer limits of the integrals that need to be performed to compute pressure and velocity from (3.6), (3.17), and (3.18).

Further contraction of the limits of integration can be achieved when the listener time t is greater than

$$t_{tail} = t_{nose} + L/U, \tag{4.6}$$

where L is the length of the aircraft. Equation (4.6) gives the time when sound from the tail of the aircraft first reaches the listener. The equation for the path of the aircraft tail in the (x', t') plot is

$$t' = (L - x')/U, \tag{4.7}$$

which replaces (4.2) in the simultaneous solution with (4.3). Two real solutions are found when $t > t_{tail}$, namely

$$x'_{2,3} = \frac{(Ut - L) \mp MU[(t - L/U)^2 - t_{nose}^2]^{1/2}}{M^2 - 1}, \tag{4.8}$$

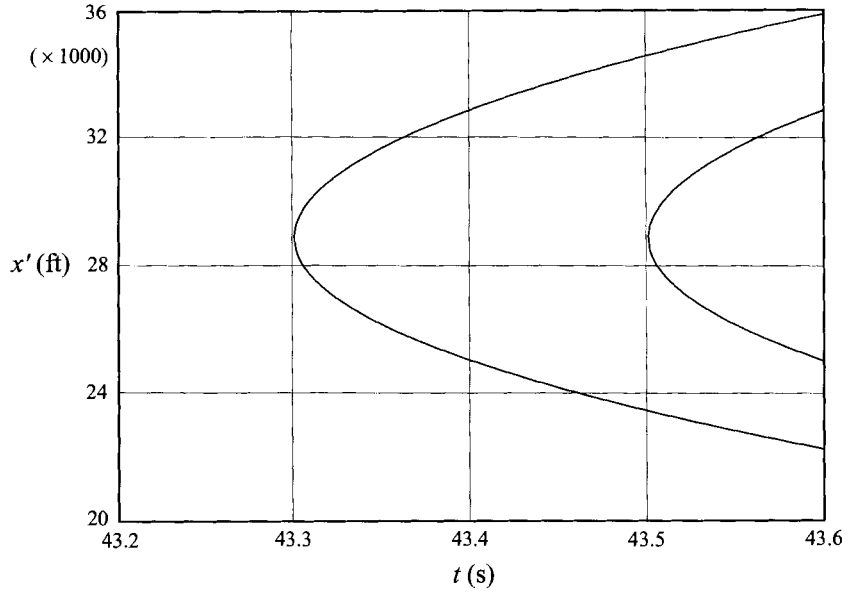

FIGURE 4. Domain of dependence for a sonic boom under conditions (4.11). Events between the two curves can influence the sonic boom heard by a listener on the ground.

which mark the intersections of the hyperbola of dependence with the upper boundary of the zone of sources.

The prescription for evaluating the solution integrals for supersonic flight is as follows. When $t < t_{nose}$, no sound has reached the listener. When $t_{nose} < t < t_{tail}$, the integrations are performed over the interval

$$x_1' \leqslant x' \leqslant x_4'. \tag{4.9}$$

Finally, when $t > t_{tail}$, the integrations are performed over two intervals,

$$x_1' \leqslant x' \leqslant x_2', \quad x_3' \leqslant x' \leqslant x_4'. \tag{4.10}$$

The limits of integration depend on sound speed, aircraft speed, aircraft length, aircraft altitude, and listener time. Figure 4 is a plot of the limits as functions of listener time for

$$c_0 = 1000 \text{ ft s}^{-1}, \quad U = 2000 \text{ ft s}^{-1}, \quad h = 50000 \text{ ft}, \quad L = 400 \text{ ft}. \tag{4.11}$$

The two curves in the plot are $x_{1,4}'$ and $x_{2,3}'$, double-valued functions of the listener time t. The region between the two curves is the comprehensive domain of dependence for the sonic boom heard by the listener.

The main lesson of figure 4 is that the domain of dependence extends over proper distances much larger than the aircraft. At $t = 43.4$ s, for example, the sonic boom amplitude encompasses events that occurred over 8000 ft of sky. At $t = 43.6$ s, the listener hears sound from two segments of sky, each about 3000 ft long, separated a distance of about 8000 ft. Typical dimensions of the domain of dependence greatly exceed the length of the aircraft.

5. Lift and drag

An enduring problem of sonic boom theory has been to explain how pressure transfers the weight of a supersonic aircraft to the ground. Equation (2.5) can be cast into integral momentum form, leaving no doubt that the integral of pressure over a rigid ground plane must equal the weight of the aircraft in steady flight regardless of

Mach number. In a memorable section of their monograph on applied aerodynamics, Prandtl & Tietjens (1934) derived the asymptotic form of ground pressure below a low-speed aircraft and showed that the pressure integrates to the weight of the aircraft. Yet an N-wave has equal positive and negative pressure lobes, so how can it support the weight of an aircraft? The answer can be found in the non-steady pressure solution (3.6).

The integral of the pressure perturbation over any horizontal plane is a force

$$F(z,t) = \int_{-\infty}^{\infty}\int_{-\infty}^{\infty} p(x,y,z,t)\,\mathrm{d}x\,\mathrm{d}y, \tag{5.1}$$

which becomes a triple integral when (3.6) is put in place of pressure. Since the integrals all extend from $-\infty$ to ∞, the order of integration does not matter, and we can replace the variables x and y with polar coordinates centred on x'. The angular integral can be performed at once, leaving integrals over x' and the polar radius

$$a = [(x-x')^2+y^2]^{1/2}. \tag{5.2}$$

Thus

$$F(z,t) = \int_0^{\infty} 2\pi a\left\{\int_{-\infty}^{\infty}\left[\rho_0\frac{\partial^2\mathscr{S}}{\partial t'^2}+\frac{z\,\partial\mathscr{F}/\partial t'}{c_0 R}+\frac{z\mathscr{F}}{R^2}\right]\frac{\mathrm{d}x'}{4\pi R}\right\}\mathrm{d}a, \tag{5.3}$$

where

$$R = (a^2+z^2)^{1/2}, \tag{5.4}$$

and

$$t' = t-R/c_0. \tag{5.5}$$

The sources $\mathscr{S}$ and $\mathscr{F}$ still depend on (x',t'), but R and t' no longer depend on x'. The integrals over x' can be performed independently of the integral over a. Define the total aircraft volume at time t',

$$V(t') = \int_{-\infty}^{\infty}\mathscr{S}(x',t')\,\mathrm{d}x', \tag{5.6}$$

and total lift

$$L(t') = -\int_{-\infty}^{\infty}\mathscr{F}(x',t')\,\mathrm{d}x' \tag{5.7}$$

for a planar lifting surface (cf. equation (2.17)). The force on the horizontal plane assumes a simpler form

$$F(z,t) = \int_0^{\infty}\left[\rho_0\frac{\mathrm{d}^2V}{\mathrm{d}t'^2}-\frac{z\,\mathrm{d}L/\mathrm{d}t'}{c_0 R}-\frac{zL}{R^2}\right]\frac{a\,\mathrm{d}a}{2R}, \tag{5.8}$$

with only a single integral remaining. The first and second terms are zero in steady flight, and the third can be integrated explicitly:

$$F(z) = -\mathrm{sgn}\,(z)\,L/2. \tag{5.9}$$

Equation (5.9) implies that pressure force on a plane below the aircraft ($\mathrm{sgn}\,(z)$ negative) is half the total lift, as expected. The other half is suction above the aircraft. If there is a ground plane at some z below the aircraft, then the pressure doubles there. The ground bears the full lift, and a reflected pressure field cancels the suction above.

The term responsible for steady lift in (5.8) derives from the term involving $\mathscr{F}/R^2$ in the integrands of the pressure solution (3.6). That term differs structurally from the other two, which fall away with distance as $1/R$. Those two terms represent acoustic waves and are fully responsible for the N-wave. The term involving $\mathscr{F}/R^2$ is weaker but more extensive at large distances, extensive enough to account for the weight of the aircraft.

Wave drag presents some interesting conceptual issues for non-steady flight. Should virtual mass effects be included in drag calculations, for example? Certainly virtual mass phenomena contribute forces in non-steady flight, but they should average to zero when the non-steady control measures are periodic. What about acoustic power

radiated from a non-steady subsonic aircraft? We may not think of such radiation as wave drag, but the power must come from somewhere and detract from power available to propel the aircraft.

A clean way to resolve such issues is to define a power-equivalent wave drag on the basis of the acoustic energy equation. To derive an energy equation from (2.4)–(2.6), we form the scalar product of (2.4) and $\boldsymbol{u}$, multiply (2.5) by p/ρ_0, eliminate ρ through (2.6), and sum the results:

$$\frac{\partial}{\partial t}\left(\frac{\rho_0|\boldsymbol{u}|^2}{2}+\frac{p^2}{2\rho_0 c_0^2}\right)+\nabla\cdot(p\boldsymbol{u})=\boldsymbol{u}\cdot\boldsymbol{f}+pq. \tag{5.10}$$

The right-hand side of (5.10) is power input per unit volume, and the left is the sum of the rate of change of energy per unit volume plus the divergence of power flux. Power delivered to the flow is a volume integral of the right-hand side,

$$P=\int_{\infty}(\boldsymbol{u}\cdot\boldsymbol{f}+pq)\,\mathrm{d}V, \tag{5.11}$$

and a power-equivalent wave drag D can be defined as P/U. By averaging the drag over a control cycle, we can show from (5.10) that

$$D=\frac{1}{U}\oiint pv\,\mathrm{d}S, \tag{5.12}$$

where the surface integral extends over an infinite cylinder those axis is the flight path, and v is the radial component of velocity given by (3.18). Use of a cylinder surrounding the flight path as a surface of integration avoids the power imparted to trailing vortices, which is infinite in slender-body theory.

6. Steady source examples

Once the limits of integration are understood, the pressure perturbation (3.6) is easy to evaluate by numerical integration. We have developed several codes to explore features of the pressure perturbation, all using Simpson's rule to integrate between the limits (4.9) and (4.10). The formulation is non-steady, but the codes apply just as well to steady flight. This section provides two examples.

Figure 5 illustrates the first example, an aircraft with a parabolic fuselage and delta wing. The fuselage and wing are assumed for simplicity to have the same length. The wing is assumed to be flat, so the lift distribution has the triangular form shown in the lower part of the figure. The triangular lift distribution derives from slender-body theory.

A steady source or lift distribution depends on the proper variables x' and t' only in the combination

$$X'=x'+Ut'. \tag{6.1}$$

We introduce a boxcar function

$$B(X')=\begin{cases}1, & 0\leqslant X'\leqslant L\\ 0, & \text{otherwise}\end{cases} \tag{6.2}$$

to account for the fact that the source and lift distributions are non-zero only over the length of the aircraft. The formula for the area distribution of a parabolic fuselage is

$$\mathscr{S}(X')=\pi B(X')\left\{4R_{max}\frac{X'(L-X')}{L^2}\right\}^2, \tag{6.3}$$

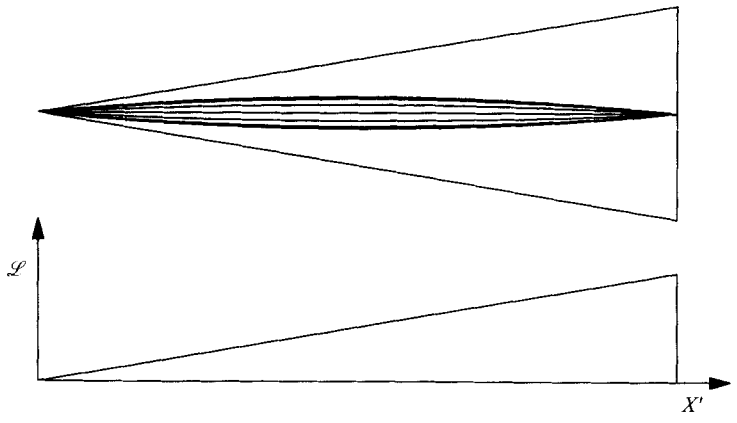

FIGURE 5. Aircraft with a parabolic fuselage and a delta wing.

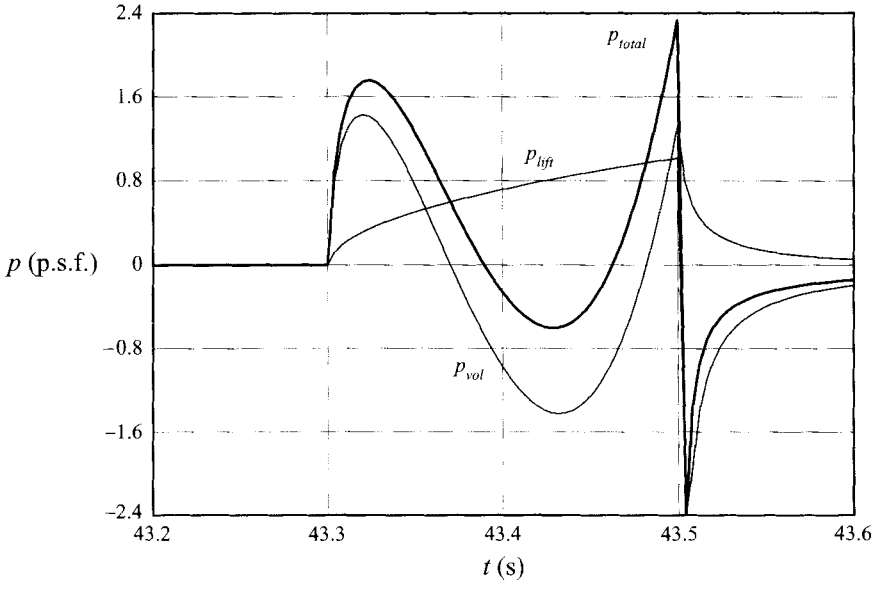

FIGURE 6. Sonic-boom wave forms for a supersonic transport with a parabolic fuselage and delta wing. Volume and lift contributions are shown separately, along with their sum.

where R_{max} is the maximum fuselage radius. The lift distribution of a delta wing has the form

$$\mathscr{L}(X') = -\mathscr{F}(X') = B(X')\frac{2WX'}{L^2}, \tag{6.4}$$

where W is the weight of the aircraft. The pressure solution (3.6) involves $\mathscr{F}$ and its first time derivative, as well as the second time derivative of $\mathscr{S}$. Because of the cusped shape of the area distribution, the derivatives of the boxcar function contribute nothing to the second derivative of (6.3), but the first derivative of (6.4) produces a delta-function singularity at $X' = L$, which needs special treatment during numerical integration.

Figure 6 shows sonic-boom wave forms computed from (3.6) times the amplification factor (3.10) to correct for density altitude and ground reflection. Flight conditions

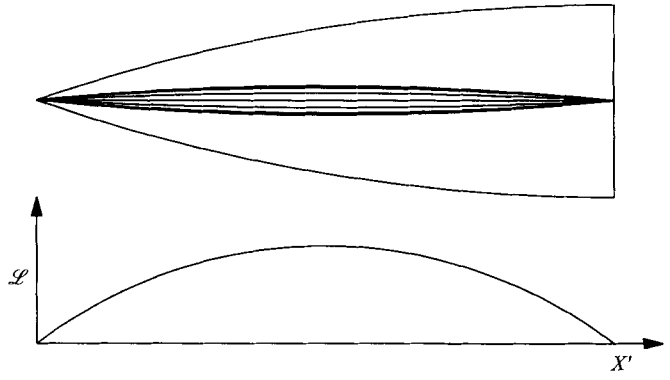

FIGURE 7. Aircraft with a half-sine fuselage and a quarter-sine wing.

include equations (4.11) plus a radius and weight appropriate for a supersonic transport:

$$R_{max} = 10 \text{ ft}, \quad W = 600\,000 \text{ lb}. \tag{6.5}$$

The thin curves in figure 6 depict pressure wave forms due to volume and lift, while the thicker curve is the total pressure perturbation. The maximum overpressure, about 2 p.s.f., is typical for sonic booms from large aircraft. The theory does not account for nonlinear propagation phenomena, so the sonic boom has only a vague resemblance to an N-wave.

Wave forms similar to those of figure 6 can be found in past work on steady supersonic flows. A plot of the pressure wave from a parabolic fuselage, for example, appears on page 92 of a monograph on aerodynamic theory by Lighthill (1960). The agreement of figure 6 with steady-state analyses helps validate our computational methods.

Our second steady example has a fuselage shaped as a half sine wave and a quarter-wave wing. When the wing is flat, slender-body theory implies that the lift distribution is a half sine wave, as seen in figure 7. The fuselage area and lift distributions have the forms

$$\mathscr{S}(X') = \pi B(X') \left\{ R_{max} \sin\left(\frac{\pi X'}{L}\right) \right\}^2, \tag{6.6}$$

$$\mathscr{L}(X') = B(X') \frac{\pi W}{2L} \sin\left(\frac{\pi X'}{L}\right). \tag{6.7}$$

Lift is symmetric around the midpoint of the wing and tapers to zero at both the apex and trailing edge. The time derivative of (6.7) produces no delta function, and no allowance need be made for a singularity at the trailing edge when performing the integrals of (3.6).

Figures 8(*a*) and 8(*b*) show pressure waves and their sources for the second steady example. Flight conditions are those of (4.11) and (6.4). The pressure wave due to volume is about the same as seen in figure 6, as is maximum overpressure. The wave form due to lift is smoother around the time waves first arrive from the trailing edge of the wing because of the absence of a lift discontinuity.

Figures 8(*a*) and 8(*b*) are a complete picture of the amplitude and origin of a sonic boom. The two figures have the same horizontal axis, listener time t. At any t, the sonic boom amplitude of figure 8(*a*) is an integral of sources along the x'-axis of figure 8(*b*). The grey levels of figure 8(*b*) indicate the sum of the three integrands in the pressure

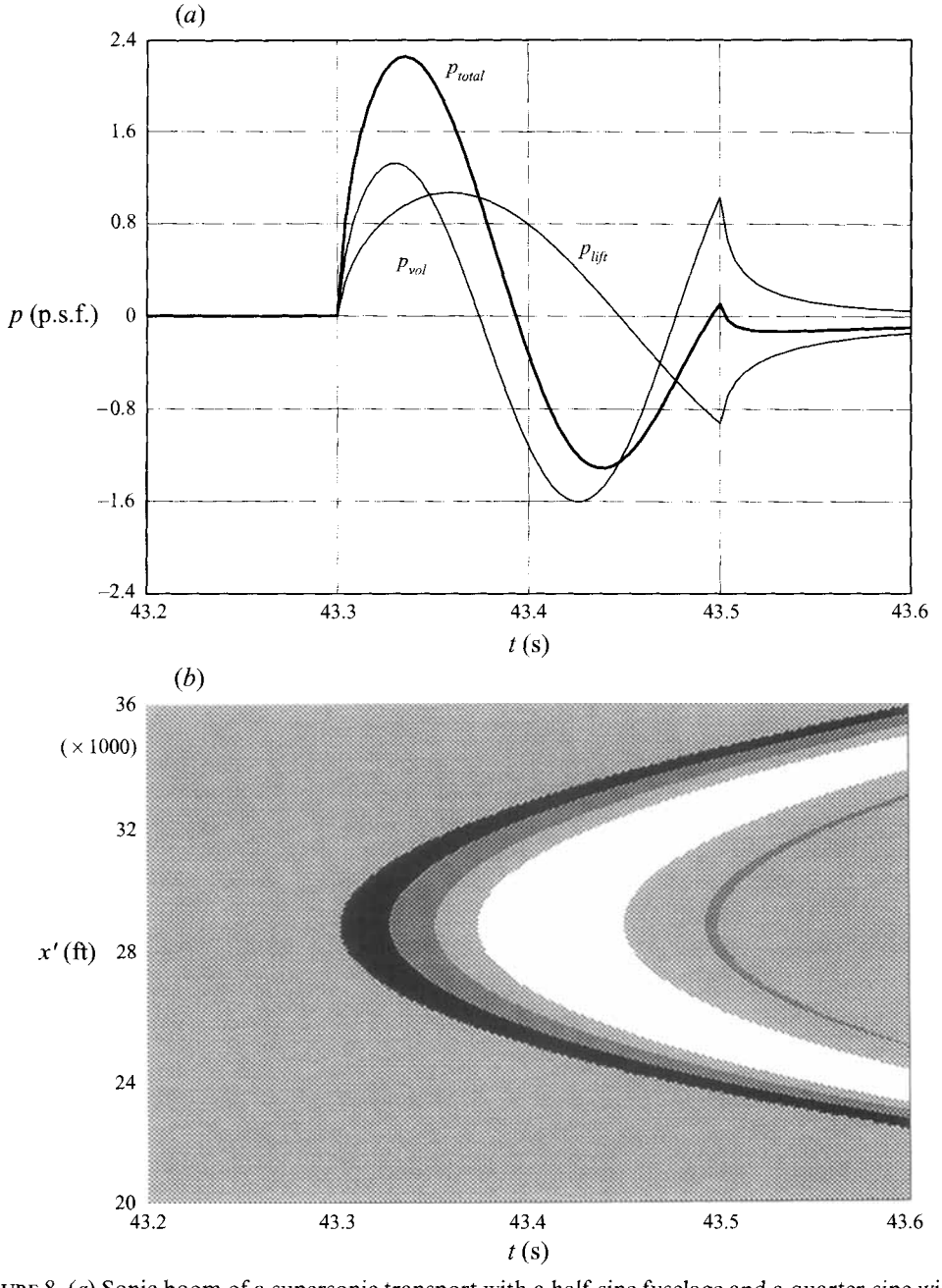

FIGURE 8. (*a*) Sonic boom of a supersonic transport with a half-sine fuselage and a quarter-sine wing. (*b*) Source distribution for the sonic boom of (*a*). The domain of dependence is the same as seen in figure 4.

solution (3.6). The region with the largest positive sources is black, intermediate positive sources are dark grey, sources near zero are light grey, and negative sources are white. Because the sources are so extensive, their actual values are small. The largest source in the domain of dependence is 0.000 34 p.s.f. ft^{-1}, and the most negative is $-0.000\,22$ p.s.f. ft^{-1}. When integrated over proper distances of 8000 ft, those sources are fully capable of producing the sonic boom amplitudes shown in figure 8(*a*).

7. Steady pressure solution

The examples of the foregoing section are steady but were computed from the non-steady pressure solution (3.6). This section shows how to transform the non-steady pressure solution into explicitly steady solutions for comparison with past theory. We resolve the pressure into volume and force terms,

$$p = p_{\mathscr{S}} + p_{\mathscr{F}}, \tag{7.1}$$

because the two terms merit somewhat different discussions.

A source moving steadily along the x'-axis is a function of the composite variable X' defined by (6.1). Pressure around a steady source is likewise a function of a composite variable

$$X = x + Ut, \tag{7.2}$$

together with the coordinates y, z transverse to the direction of travel. When variables X and X' are included in (3.5) and (3.6), the pressures due to volume and body force take the forms

$$p_{\mathscr{S}}(X, y, z) = \rho_0 U^2 \int_{-\infty}^{\infty} \mathscr{S}''(X') \frac{\mathrm{d}x'}{4\pi R}, \tag{7.3}$$

$$p_{\mathscr{F}}(X, y, z) = -\frac{\partial}{\partial z} \int_{-\infty}^{\infty} \mathscr{F}(X') \frac{\mathrm{d}x'}{4\pi R} = z \int_{-\infty}^{\infty} \left[\frac{M\mathscr{F}'(X')}{R} + \frac{\mathscr{F}(X')}{R^2} \right] \frac{\mathrm{d}x'}{4\pi R}, \tag{7.4}$$

where

$$R = [(x-x')^2 + r^2]^{1/2} \quad \text{and} \quad r = (y^2+z^2)^{1/2}. \tag{7.5}$$

The first member of (7.4) comes from the pressure solution (3.5) with the z-derivative outside the integral, while the second member comes from (3.6) with the derivative inside. Primes on the area and force distributions indicate differentiations with respect to their argument. The integrals may seem to retain a dependence on x, but that is not so. Only the difference $(x-x')$ appears in the integrands, and the difference could be used as a dummy variable of integration.

To recover past results for steady sonic booms, we have only to substitute X' for x' as the variable of integration (7.3) and (7.4). The two variables are related by definition (3.3) of proper time, which may be written in the forms

$$\begin{aligned} X - X' &= x - x' + U(t-t') \\ &= x - x' + MR. \end{aligned} \tag{7.6}$$

The latter can be solved for $(x-x')$ as a function of $(X-X')$.

Figure 9 illustrates the relation between X' and x' for the case of supersonic flight. X' has a maximum,

$$X' \leqslant X - Br, \tag{7.7}$$

where

$$B = (M^2-1)^{1/2}. \tag{7.8}$$

The maximum is negative where X lies ahead of the Mach cone whose apex is the nose of the aircraft. There are area and lift distributions are zero for all x', and the pressure perturbation is zero. Otherwise, each value of X' corresponds to two values of x', and contributions from both must be included in the transformed integral.

The Jacobian of the transformation proves to be

$$\left| \frac{\mathrm{d}x'}{\mathrm{d}X'} \right| = \frac{R}{\lambda}, \tag{7.9}$$

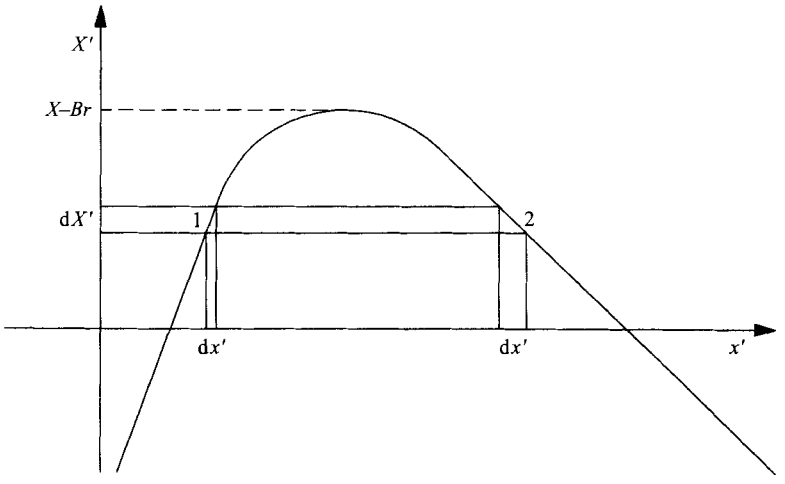

FIGURE 9. Relationship of the alternative integration variables X' and x'.

where

$$\lambda = [(X-X')^2 - B^2r^2]^{1/2}. \tag{7.10}$$

The Jacobian (7.9) applies to each of the two values of x' at a single X', so a term of an integral over x' produces two terms in the integral over X'.

To compare our results with earlier work, we need to assume that the volume and force distributions and the derivative of the volume distribution are zero ahead of the aircraft and at its nose:

$$\mathscr{S}(X') = 0, \quad \mathscr{S}'(X') = 0, \quad \mathscr{F}(X') = 0 \quad \text{for} \quad X' \leqslant 0. \tag{7.11}$$

Transformation of (7.3) is simple,

$$p_{\mathscr{S}} = \rho_0 U^2 \int_0^{X-Br} \mathscr{S}''(X') \frac{\mathrm{d}X'}{2\pi\lambda}, \tag{7.12}$$

and reproduces the known solution for pressure due to volume displacement around a body in steady supersonic flight. The integral can be found in various references (e.g. Whitham 1974) but is most commonly seen in an asymptotic form valid far from the flight path.

Transformation of the first member of (7.4) is also simple,

$$p_{\mathscr{F}} = -\frac{\partial}{\partial z} \int_0^{X-Br} \mathscr{F}(X') \frac{\mathrm{d}X'}{2\pi\lambda}, \tag{7.13}$$

but the result is not usually seen with the derivative outside the integral. Straightforward differentiation fails, moreover, because the integrand is singular at the upper limit. A transformation of variables removes the singularity:

$$X' = X - Br\cosh\xi, \tag{7.14}$$

and the subsequent differentiation produces a formula that can be compared with the theory of lifting slender bodies in steady supersonic flight (Tsien 1938):

$$p_{\mathscr{F}} = \frac{Bz}{2\pi r} \int_0^{\cosh^{-1}(X/Br)} \mathscr{F}'(X - Br\cosh\xi)\cosh\xi \,\mathrm{d}\xi. \tag{7.15}$$

We recover a formula with the same structure as (7.12) by transforming back to the variable X':

$$p_{\mathscr{F}} = \frac{z}{r^2}\int_0^{X-Br} \mathscr{F}'(X')(X-X')\frac{\mathrm{d}X'}{2\pi\lambda}. \tag{7.16}$$

Tsien's paper concerns flow around slender bodies of revolution, so we must use (2.18) to relate the distributions of body force $\mathscr{F}$ and lift $\mathscr{L}$. In steady flight, the lift distribution satisfies the formula

$$\mathscr{L} = \rho_0 U^2 \sin\alpha \frac{\mathrm{d}\mathscr{S}}{\mathrm{d}X}, \tag{7.17}$$

where α is angle of attack. Tsien presents a formula for potential rather than pressure, but the two are related by an integral of the steady Euler equation,

$$p = -\rho_0 U \frac{\partial\phi}{\partial X}. \tag{7.18}$$

Our solution (7.15) for pressure due to lift agrees with Tsien's solution (4) for potential together with (2.18), (7.17), and (7.18).†

When the second member of (7.4) is transformed into an integral over X', a cumbersome formula results:

$$p_{\mathscr{F}} = z\int_0^{X-Br}\left\{\frac{M^2(X-X')\mathscr{F}'(X')}{(X-X')^2+r^2} + \frac{[(M^2+1)(X-X')^2 - B^2r^2]\mathscr{F}(X')}{[(X-X')^2+r^2]^2}\right\}\frac{\mathrm{d}X'}{2\pi\lambda}. \tag{7.19}$$

Solutions (7.16) and (7.19) can be shown to be equivalent by proving that

$$\frac{\mathrm{d}}{\mathrm{d}X'}\left\{\frac{M^2(X-X')}{[(X-X')^2+r^2]\lambda} - \frac{(X-X')}{r^2\lambda}\right\} = \frac{(M^2+1)(X-X')^2 - B^2r^2}{[(X-X')^2+r^2]^2\lambda} \tag{7.20}$$

and integrating (7.19) by parts.

The solution (7.16) looks much simpler than (7.19), so why bother with (7.19) at all? The answer is that the two terms of (7.19) represent distinct components of the pressure field, and the distinction is worth taking into account. The first term is a propagating acoustic wave, the N-wave of sonic boom fame. The second terms falls away too fast to project acoustic power. It is bounded by the Mach cone but otherwise behaves like a near field. The second term alone contributes to the pressure integral (5.19) and transfers the weight of the aircraft to the ground.

Although it is solely responsible for weight transfer, the second term of (7.19) is much smaller than the first near the Mach cone. An asymptotic analysis of (7.16) could easily miss the phenomenon of weight transfer, though it is a rigorous consequence of the linear acoustics equations, as well as the nonlinear Euler equations. Separate asymptotic analyses of the two terms of (7.19) illuminate the influence of lift on the N-wave and the transfer of weight to the ground.

8. Steady lift and drag

The second term of (7.19) is easy to evaluate far from the flight path. $\mathscr{F}(X')$ is non-zero only from 0 to L, regardless of the upper limit $X-Br$. As r becomes large, X' becomes negligible in the factors multiplying $\mathscr{F}(X')$ everywhere that $\mathscr{F}(X')$ is non-zero.

† There is a small difference in that the sign on the right of Tsien's equation (5) needs to be changed, as does the sign on the right of (7). Δp in (6) must be interpreted as the pressure difference between the lower and upper surfaces of the body, rather than 'the difference between the pressure at the surface of the body and the undisturbed flow'. Otherwise the relation between pressure and potential in (6) differs by a factor of 2, as does the domain of angular integration.

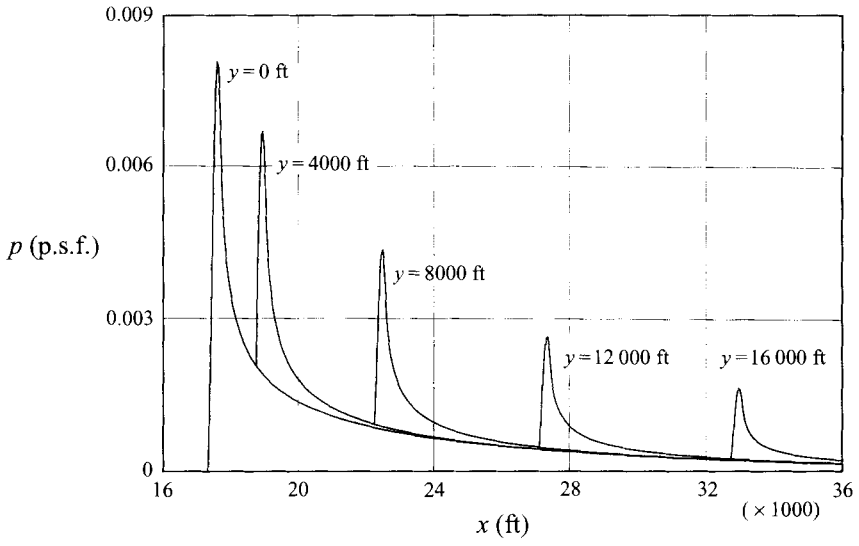

FIGURE 10. Ground pressure behind the Mach cone at various lateral distances from the flight path.

The second term can be integrated to yield an asymptotic pressure formula proportional to total lift L,

$$p_{\mathscr{F}} \to \frac{h[(M^2+1)X^2 - B^2r^2]L}{2\pi(X^2+r^2)^2(X^2-B^2r^2)^{1/2}}, \tag{8.1}$$

valid behind the Mach cone where $X > Br$. Equation (8.1) is singular at $X = Br$, but the singularity is integrable. The integral over a horizontal plane below the aircraft is $L/2$, and ground reflection doubles the integral to the full lift of the aircraft. Equation (8.1) is the analogue of the famous asymptotic formula for the ground pressure of a low-speed aircraft (Prandtl & Tietjens 1934, pp. 186–188). Of course (8.1) exhibits no hint of the N-wave to be found by evaluating the first term of (7.19) far from the flight path.

Equation (8.1) is hard to plot because of the singularity at the Mach cone, but figure 10 shows exact values of the same pressure term for our aircraft with sinusoidal fuselage radius and lift distributions flying at Mach 2 and an altitude of 10000 ft. The figure shows ground pressures at several lateral locations to indicate the extent of the pressure footprint. Not shown are the much larger sonic boom pressures near the Mach cone.

Our concept of power-equivalent wave drag may seem exotic, but it reduces to the classical definition of wave drag when the flow is steady. With the substitution of (7.1), the x-component of the acoustic momentum equation (2.5) takes the form

$$\partial(\rho_0 Uu + p)/\partial X = 0, \tag{8.2}$$

when no body force is directed along the x-axis. We conclude that the term in brackets is zero, and the drag formula (5.12) becomes a surface integral of momentum flux:

$$D = -\rho_0 \oiint uv \, \mathrm{d}S. \tag{8.3}$$

Equation (8.3), together with asymptotic formulae for the longitudinal and radial velocity components, reproduces classical results for wave drag of slender bodies in supersonic flight (von Kármán & Moore 1932).

9. Periodic sources

The rest of this paper concerns periodic moving sources of the sort that might be used to control sonic booms. Of course any non-steady sources aboard supersonic transports would face formidable constraints. We cannot seriously contemplate non-steady fuselage shape changes, but perhaps leading edges with 'smart skins' could periodically alter the longitudinal lift distribution. The total lift and centre of lift could remain constant, but the lift distribution could 'slosh' in and out from the middle of the aircraft to the nose and tail. Periodic manoeuvres without shape changes are unattractive but theoretically possible. Without altering its flight path, an aircraft could 'surge' periodically in speed. Both 'slosh' and 'surge' are examples of periodic moving sources.

Important information about active sonic boom control can be obtained from a general definition of periodic moving sources, without recourse to specific examples. The definition proves to be curiously subtle. In the context of slender-body theory, any source is a function of the proper variables x', t'. A less obvious variable is the phase τ of the clock that times the periodic control measures aboard the aircraft. Any conclusions about active sonic boom control should be independent of the phase of the aircraft clock. Put another way, the conclusions should not depend on the location x of a listener under the flight path.

We thus assume that a periodic moving source is a function q of three variables (x', t', τ) including the phase of the control clock. 'Moving' means that x' and t' combine into a single variable so that

$$q(x', t', \tau) = f(x' + Ut', t' - \tau). \tag{9.1}$$

'Periodic' means that q does not change when the phase increases by a time equal to the period T of the control system:

$$q(x', t', \tau + T) = q(x', t', \tau). \tag{9.2}$$

Equations (9.1) and (9.2) fully define a periodic moving source.

The source has a phase average

$$Q(x', t', \tau) = \frac{1}{T}\int_{\tau}^{\tau+T} q(x', t', \tau')\,\mathrm{d}\tau'. \tag{9.3}$$

The phase average appears to be a function of the three variables (x', t', τ), but we can easily show from (9.1)–(9.3) that

$$\frac{\partial Q}{\partial \tau} = 0, \quad \frac{\partial Q}{\partial t'} - U\frac{\partial Q}{\partial x'} = 0. \tag{9.4}$$

Thus the phase average is a function of one variable only,

$$Q(x', t', \tau) = Q(x' + Ut'), \tag{9.5}$$

and has the same form as a steady moving source. Phase averaging smears the source distribution along a direction parallel to the boundaries of the zone of sources.

Phase averaging commutes with the spatial integrals of solution (3.6) for the pressure perturbation. Thus the phase-average pressure perturbation is the same as a pressure perturbation from the phase-average source, and the phase-averaged source is the same as a steady moving source. *The phase-averaged sonic boom is the same as the sonic boom of a steady aircraft whose source distributions are phase averages of sources under active control.*

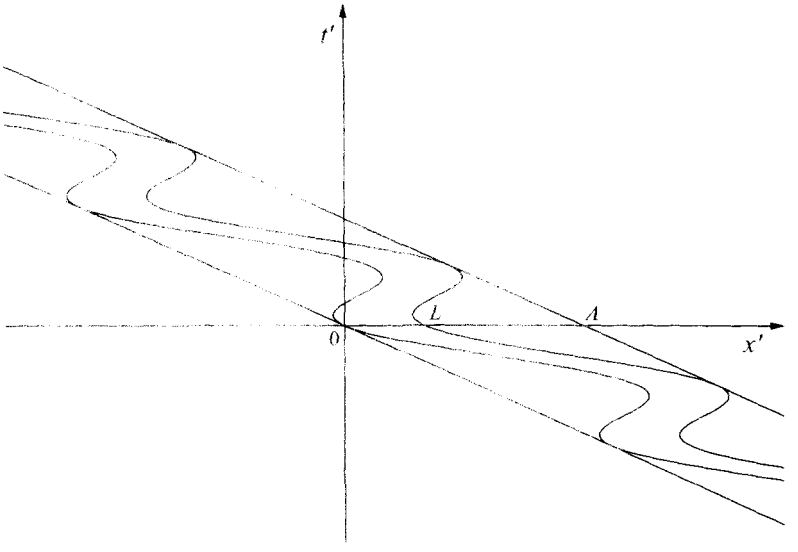

FIGURE 11. Zone of sources with periodic surge. Surge stretches the zone from the aircraft length L to some larger dimension Λ.

Can active control have any effect on the average sonic boom? The answer may be no for control methods like slosh but clearly is yes for manoeuvres like surge. Figure 11 shows how surge alters the extent of the zone of sources, stretching the zone from the aircraft length L to a greater length Λ, the sum of aircraft length plus twice the amplitude of surge. The phase-average theorem (9.6) still applies, but the phase-averaged source is an aircraft of length Λ rather than L.

10. Periodic slosh

Our first example of a periodic source is 'slosh', a longitudinal flow of lift back and forth from the middle of the aircraft to the nose and tail. An aircraft with three lifting surfaces could implement slosh by oscillating control surfaces at the three trailing edges, with the canard and tail synchronized and the wing 180° out of phase. Alternatively, an elongated delta or quarter-sine wing could have piezoelectric leading edges capable of bending into S shapes, thereby altering the longitudinal distribution of angle of attack.

We retain the sinusoidal fuselage radius of (6.6) but add a three-halves sine wave to the lift distribution (6.7):

$$\mathscr{L}(x', t') = B(X')\frac{\pi W}{2L}\left[(1-\beta)\sin\left(\frac{\pi X'}{L}\right)+3\beta\sin\left(\frac{3\pi X'}{L}\right)\right]. \tag{10.1}$$

The lift distribution (10.1) is always symmetrical around the middle of the aircraft, so the centre of lift never changes. The factors $(1-\beta)$ and 3β are selected so the total lift is constant as well. β determines whether the lift distribution is peaked in the middle or peaked toward the nose and tail. The formula

$$\beta = \beta_0 + \beta_1 \sin(2\pi f t' + \phi) \tag{10.2}$$

specifies a mean allocation of lift to the three-halves sine term as well as a periodic allocation of frequency f and phase ϕ in radians. The mean allocation is proportional to β_0 and the periodic allocation to β_1.

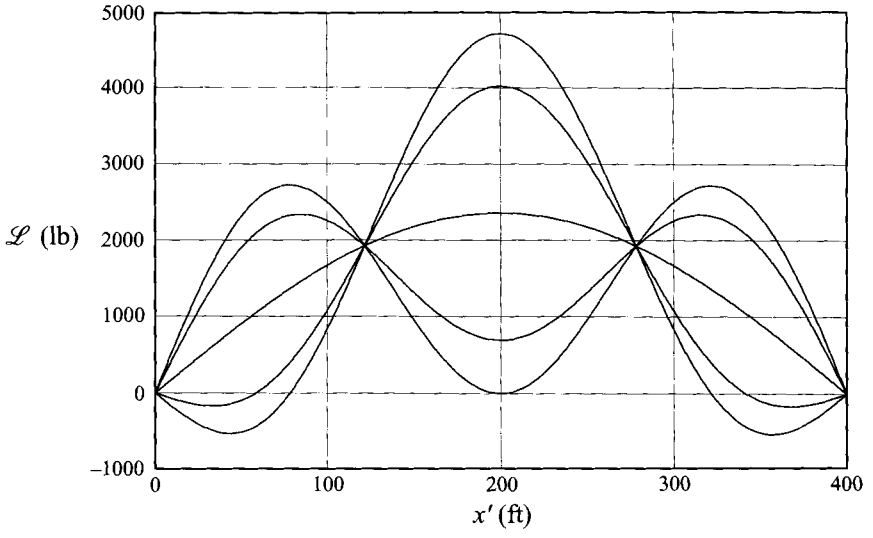

FIGURE 12. Longitudinal lift distribution under extreme slosh for eight evenly spaced phases; $\beta_0 = 0$, $\beta_1 = 0.25$.

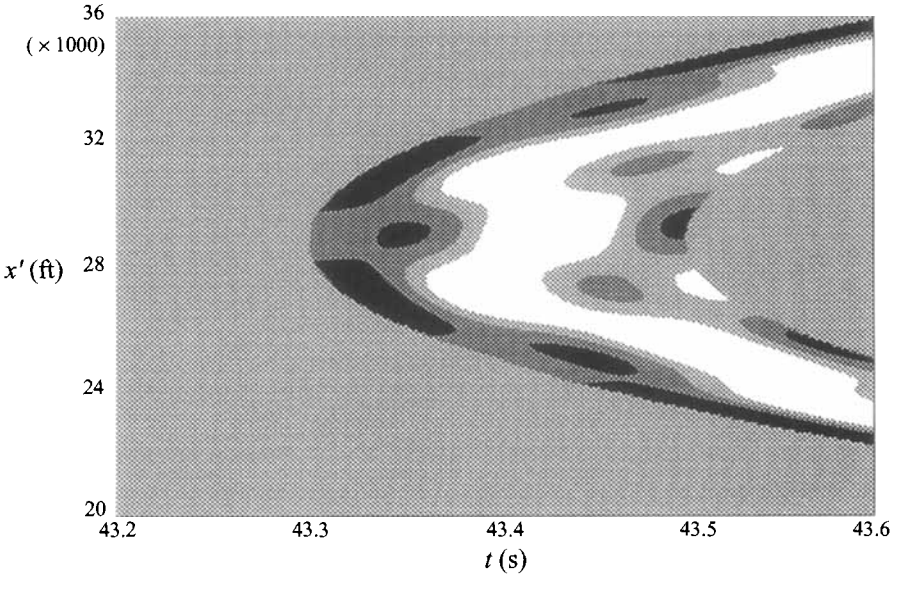

FIGURE 13. Source distribution under extreme slosh at a frequency of 0.5 Hz.

Figure 12 displays lift distributions for

$$\beta_0 = 0, \quad \beta_1 = 0.25. \tag{10.3}$$

The aircraft parameters are those of (4.11) and (6.5), while the proper time t' is zero in all cases. Lift plots for eight evenly spaced phases are shown: $\phi = 0°$, $+5°$, $90°$, ... Three of the plots overlap others. The amount of slosh is seen to be extreme. The lift at the middle of the aircraft periodically falls to zero and becomes double the mean value. We should not expect to attain greater lift variability in practice.

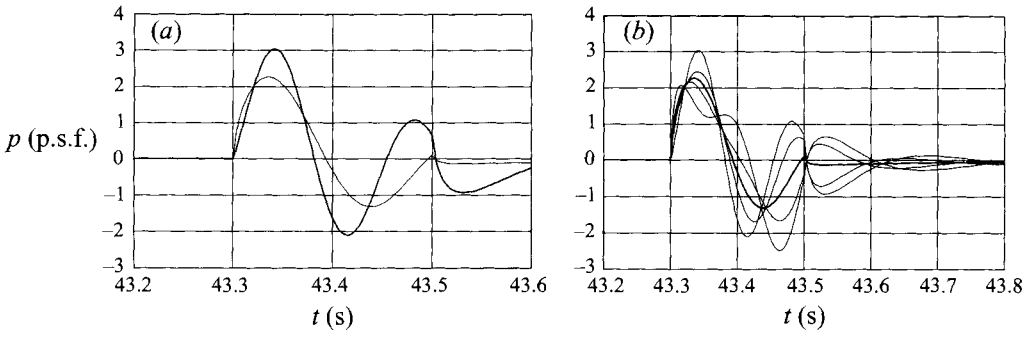

FIGURE 14. (*a*) Sonic boom from a sloshed lift distribution. The light line depicts the sonic boom for steady lift. (*b*) Sonic booms from four phases of the slosh cycle, together with their average shown as a darker curve. The average is the same as the boom from the steady source of (*a*).

Figure 13 shows the source distribution that results when the slosh is imposed at a frequency f of 0.5 Hz, with a phase ϕ of zero. Extreme slosh has dramatic effects on the source distribution, as may be seen by comparing grey levels of figures 13 and 8(*b*). Convoluted source regions have replaced the clean arcs of the steady source example.

Figures 14(*a*) and 14(*b*) display sonic booms arising from periodic slosh. The darker curve in figure 14(*a*) is the boom at zero phase, while the lighter curve is the boom of the steady source example, reproduced from figure 8(*a*). The lighter curves of figure 14(*b*) are booms at four phases of the slosh cycle: $\phi = 0°$, 90°, 180° and 270°. The darker curve is the average of the four and is the same as the boom from the steady source, in conformity with the phase-average theorem of §9. We conclude from the plots that slosh alters the boom profoundly but does not reduce its pressure level.

11. Periodic surge

Our second example of a periodic source is 'surge', a periodic acceleration of the aircraft along its flight path. In principle, engine thrust variations could implement surge. A deliberately excited phugoid oscillation could do so also, with the complication of small periodic changes of altitude. We recommend neither mode of implementation for commercial supersonic transports!

The half-sine fuselage and quarter-sine wing of (6.6) and (6.7) suffice without change to demonstrate surge phenomenology. What must change is the definition of the composite proper coordinate X'. In place of (6.1), we require that

$$X' = x' + Ut' - \tfrac{1}{2}(\Lambda - L)[1 - \cos(2\pi f t' + \phi)], \tag{11.1}$$

where f is surge frequency and ϕ is an arbitrary phase. Surge is a sinusoidal motion superposed on the mean translatory motion of the aircraft. The amplitude of sinusoidal motion is $(\Lambda - L)/2$, where Λ is the length of the zone of sources shown in figure 11.

Figure 15 shows the source distribution derived from (6.6), (6.7), and (11.1) for a frequency of 0.5 Hz and zero phase. The aircraft parameters and flight conditions are from (4.11) and (6.5) as usual, while the amplitude of the surface is assumed to be 400 ft, the same as the length of the aircraft. The length of the zone of sources is 1200 ft, three times longer than the aircraft.

The sources in figure 15 are no longer compact within the nominal zone of sources. They snake back and forth between the boundaries of the zone, creating a stretched

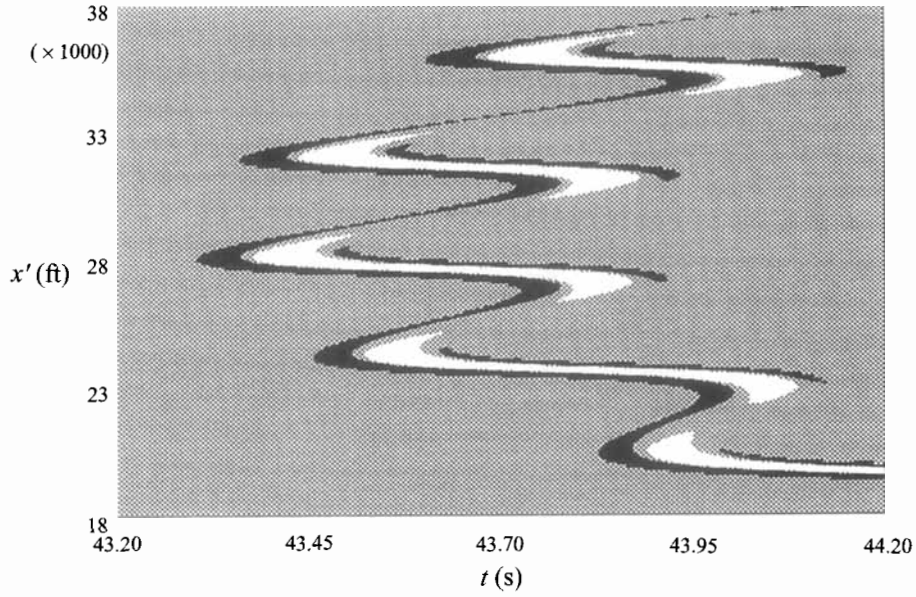

FIGURE 15. Source distribution for surge at a frequency of 0.5 Hz.

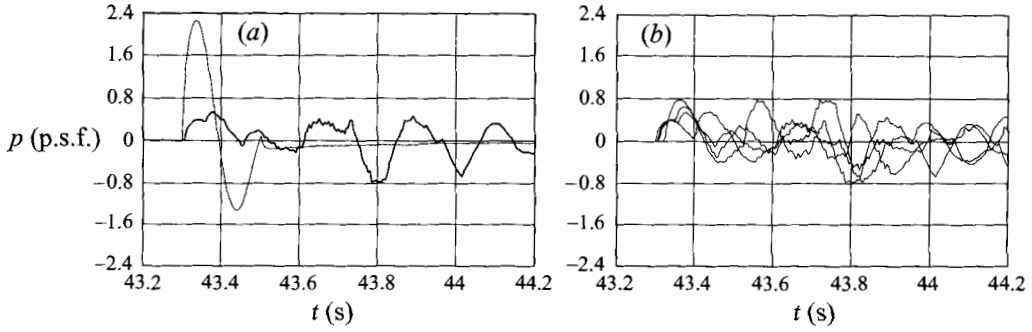

FIGURE 16. (*a*) Sonic boom from an aircraft subject to extreme periodic surge. The lighter curve depicts the boom without surge. (*b*) Sonic booms from four phases of the surge cycle.

and attenuated virtual source of sound. Sonic booms from the surging aircraft are similarly stretched and attenuated, as shown in figures 16(*a*) and 16(*b*). The sonic boom of figure 8(*a*) has collapsed into waves of low amplitude resembling broadband noise. The waves seem oddly complicated in view of their origin from a simple aircraft undergoing a simple sinusoidal surge.

Unfortunately the assumed surge amplitude is anything but practical. Position oscillates with an amplitude of 400 ft and frequency of 0.5 Hz. The amplitude of speed oscillations is 1257 ft s^{-1}, so the speed varies from 743 ft s^{-1} to 3257 ft s^{-1} in the course of a cycle. Acceleration oscillations have an amplitude of 3948 ft s^{-2}, about 123 times the acceleration due to gravity.

The speed and acceleration amplitudes diminish as the frequency falls, but so does the efficacy of surge as a means of reducing sonic boom intensity. At a frequency of 0.1 Hz, the amplitude of acceleration is 'only' 4.9 times gravity, but the sonic boom is hardly changed from the case of steady flight. Surge with more moderate

accelerations shifts the boom back and forth without chopping it to pieces, like the fragmented booms of figures 16(*a*) and 16(*b*). The phase-averaged boom is still weak, but the weakness reflects only boom displacements, not intensity reductions that a listener would notice.

12. Conclusions

Non-steady acoustics and slender-body theory serve well as bases for a linear theory of sonic booms. The non-steady solution for sonic boom pressure is easy to understand and compute, a little easier than the equivalent steady solution, even when the sources are steady. Lift evolves naturally in the non-steady formulation and gives rise to separate terms that account for sonic booms and for transfer of aircraft weight to the ground.

A major conclusion of non-steady theory is that the source of a sonic boom is much larger than the aircraft. For an aircraft flying at an altitude of 50000 ft, the source region at any instant is typically 8000 ft long. The sonic boom emanates from an extensive region of sky, a kind of synthetic aperture acoustic antenna. By exploiting the dimension of time, an aircraft can alter the source distribution along the synthetic aperture antenna and subject the sonic boom to active control.

A theorem limits the options for effective active control, at least within the realm of linear theory. The theorem states that the phase-averaged sonic boom is the same as the sonic boom of a steady aircraft whose source distributions are phase averages of sources under active control. The only way the aircraft can reduce the phase-average sonic boom is by manoeuvring to enlarge the source region beyond the bounds defined by flight at constant velocity.

We assume that fuselage shape must be constant and consider two means of active sonic boom control called 'slosh' and 'surge'. Slosh is periodic contraction and expansion of the longitudinal lift distribution, with total lift and centre of lift held constant. Surge is a periodic aircraft manoeuvre, not a change of shape. The aircraft speed surges faster and slower along an unchanged flight path.

Slosh of sufficient magnitude has a dramatic effect on sonic booms, but the phase-average theorem precludes any average change of boom strength. If boom amplitude decreases at one point below the flight path, it must increase at another. Surge, by contrast, can reduce sonic boom amplitudes everywhere below the flight path and transform the boom into seemingly random noise. The accelerations needed to produce that happy outcome seem much too large to be practical, but the fact that surge can reduce sonic booms to rumbles is surprising and intriguing.

We conclude that active sonic boom abatement is possible but not necessarily practical. There could be some means beyond slosh and surge that can reduce sonic booms actively without imposing impractical burdens on the aircraft. Nonlinear propagation could also have a bearing on the ultimate utility of active sonic boom control. A boom heard on the ground comes from a wide swathe of sky. Some points of origin are strong with active control, and others are weak. The fact that the boom coalesces from strong and weak sources may influence the formation and propagation of shock waves.

Another nonlinearity may be important: one involving sources rather than propagation. An aircraft vortex wake is a nonlinear source of pressure perturbations superposed on the pressure perturbations from the fuselage and wing. Vortex boom phenomena would be easy to include in non-steady sonic boom theory and could have some bearing on steady booms as well.

This work was sponsored by the NASA Langley Research Center. We are grateful for the support from NASA Langley and for the encouragement of Dennis Bushnell, Christine Darden, and Daniel Baize.

REFERENCES

COLE, J. D. 1953 Note on non-stationary slender body theory. *J. Aero Sci.* **20**, 798–799.

CROW, S. C. 1969 Distortion of sonic bangs by atmospheric turbulence. *J. Fluid Mech.* **37**, 529–563.

GARRICK, I. E. & MAGLIERI, D. J. 1968 A summary of results on sonic-boom pressure-signature variations associated with atmospheric conditions. *NASA TN* D-4588.

GOLDSTEIN, M. E. 1976 *Aeroacoustics*, pp. 45–53. McGraw-Hill.

HAYES, W. D. 1954 Pseudotransonic similitude and first-order wave structure. *J. Aero. Sci.* **21**, 721–730.

HAYES, W. D. 1971 Sonic boom. *Ann. Rev. Fluid Mech.* **3**, 269–290.

HAYES, W. D., HAEFELI, R. C. & KULSTRUD, H. E. 1969 Sonic boom propagation in a stratified atmosphere with computer program. *NASA Contractor Rep.* CR-1299.

KÁRMÁN, T. VON & MOORE, N. B. 1932 Resistance of slender bodies moving with supersonic velocities with special reference to projectiles. *Trans. ASME* **54**, 303–310.

LAMB, H. 1933 *Hydrodynamics*, 6th Edn. Cambridge University Press.

LANDAU, L. 1945 On shock waves at large distances from the place of their origin. *J. Phys. USSR* **9**, 496.

LIGHTHILL, M. J. 1952 On sound generated aerodynamically. I. General theory. *Proc. R. Soc. Lond.* A **211**, 564–587.

LIGHTHILL, M. J. 1960 *Higher Approximations in Aerodynamic Theory*. Princeton University Press.

PRANDTL, L. & TIETJENS, O. G. 1934 *Applied Hydro- and Aeromechanics*. Dover.

SEEBASS, R. 1970 Nonlinear acoustic behavior at a caustic. *Third Conf. on Sonic Boom Research, NASA SP*-255, pp. 87–120.

TSIEN, H. S. 1938 Supersonic flow over an inclined body of revolution. *J. Aero. Sci.* **5**, 480–483.

WHITHAM, G. B. 1956 On the propagation of weak shock waves. *J. Fluid Mech.* **1**, 290–318.

WHITHAM, G. B. 1974 *Linear and Nonlinear Waves*. John Wiley.